

# Characterization of Pan-Based Gel Electrolytes. Electrochemical Stability and Lithium Cyclability

G. Dautzenberg, F. Croce, S. Passerini, and B. Scrosati\*

Dipartimento di Chimica, Università di Roma La Sapienza, Rome, Italy

Received October 26, 1993. Revised Manuscript Received February 11, 1994\*

The electrochemical characteristics of gel electrolytes, formed by the immobilization of propylene carbonate/ethylene carbonate PC/EC solutions containing various LiX lithium salts in poly(acrylonitrile) PAN matrix, have been investigated. Comparisons with parent liquid electrolytes (EC/PC-LiX) have been made. The results based on cyclic voltammetry and lithium plating-stripping tests suggest that the most suitable applicability of this kind of electrolytes is in the so-called rocking chair devices, such as lithium ion batteries and electrochromic windows.

## Introduction

The PAN-based gel electrolytes are presently considered of interest as separators in rechargeable lithium batteries. The main motivation for this expectation is the high conductivity at ambient and subambient temperature. Indeed, these electrolytes have conductivity of the order of  $10^{-3}$  S  $\text{cm}^{-1}$  at 25 °C and of  $10^{-4}$  S  $\text{cm}^{-1}$  at -20 °C.<sup>1-3</sup> However, high conductivity, although an important factor, is not sufficient to make a given electrolyte suitable for battery applications. Also the electrochemical stability window and the compatibility with the electrode materials are key parameters, especially in terms of reliability and rechargeability.

Surprisingly, while a few papers have been published on the transport properties of these gel electrolytes, very little attention has been so far dedicated to their electrochemical stability and to their interfacial properties. Therefore, it has appeared to us of importance to fill this gap, and in this work we report the result of a detailed investigation of the anodic and the cathodic decomposition limits of various PAN-based electrolyte samples, as well as of the characteristics of the lithium plating-stripping process in related electrochemical cells.

## Experimental Section

All the preparation procedures of the gel electrolytes and the related electrochemical measurements were carried out in an argon-filled glovebox. The chemical products used were purified and dried. PAN (Aldrich, reagent grade), lithium perchlorate ( $\text{LiClO}_4$ , Fluka, high-purity grade), and trifluoromethanesulphonamide ( $\text{LiN}(\text{CF}_3\text{SO}_2)_2$ , 3 M, high-purity grade) were dried under vacuum at 80, 60, and 110 °C, respectively. Lithium hexafluoroarsenate ( $\text{LiAsF}_6$ , 3M product) was used as received. Ethylene carbonate, EC (Fluka, reagent grade) was distilled under reduced pressure. Purified EC was added to propylene carbonate, PC (Fluka, high-purity grade), and the resulting mixture was finally dried over molecular sieves.

The gelification procedure consisted of three consecutive steps. Initially, the selected lithium salt (LiX) was dissolved in the

PC/EC mixture at room temperature. The second step involved the swelling of PAN in the PC/EC-LiX solution, which was then completed by heating the solution at about 100-110 °C, under continuous stirring for 1 h. Finally, the gel was cast between two glass plates. The insertion of metallic spacers between the glass plates allowed us to obtain samples of defined thickness (100-150  $\mu\text{m}$ ). The gel electrolyte membranes so prepared had a plasticlike consistency with a wet surface appearance, the latter effect being due to the fact that a fraction of liquid solvent (PC and EC) is not interacting directly with the polymer chain.<sup>4</sup> The degree of transparency of the membranes depends on the nature of the lithium salt used and on the content of PAN. The most transparent samples were obtained when using  $\text{LiClO}_4$  at lower PAN content. On the contrary, samples containing the imide salt appeared opaque with a light yellow coloration.

Various gel electrolyte membranes having different compositions were prepared. The samples examined in this work had the following molar ratios:

Sample GE-1: PAN 16/PC 23/EC 56.5/LiX 4.5; X =  $\text{ClO}_4^-$ ,  $\text{AsF}_6^-$ ,  $\text{N}(\text{CF}_3\text{SO}_2)_2^-$ .

Sample GE-2: PAN 16/PC 37/EC 42.5/LiX 4.5; X =  $\text{ClO}_4^-$ .

Sample GE-3: PAN 21/PC 34.75/EC 40/LiX 4.25; X =  $\text{ClO}_4^-$ ,  $\text{AsF}_6^-$ ,  $\text{N}(\text{CF}_3\text{SO}_2)_2^-$ .

Sample GE-4: PAN 21/PC 33/EC 38/ $\text{LiClO}_4$  8; X =  $\text{ClO}_4^-$ .

Sample GE-5: PAN 25/PC 33/EC 38/ $\text{LiClO}_4$  4; X =  $\text{ClO}_4^-$ .

While the molar ratios of the parent liquid electrolytes were as follows:

Sample LE-1: PC 27.4/EC 67.3/LiX 5.3; X =  $\text{ClO}_4^-$ ,  $\text{AsF}_6^-$ ,  $\text{N}(\text{CF}_3\text{SO}_2)_2^-$ .

Sample LE-2: PC 44/EC 50.6/LiX 5.4; X =  $\text{ClO}_4^-$ ,  $\text{AsF}_6^-$ ,  $\text{N}(\text{CF}_3\text{SO}_2)_2^-$ .

All the electrochemical tests on these samples were performed in a three-electrode cell in which a lithium disk was used as the counterelectrode, and a lithium strip was the reference electrode.

In the case of the liquid electrolyte cells, the reference electrode was placed in the proximity of the working electrode, while for the solid electrolyte cells the reference electrode was placed between two adjacent disks of the gel electrolyte. Stainless steel (SS 304), nickel, carbon fiber, and glassy carbon, respectively, were used as working electrodes.

The experimental setup was composed of a scanning potentiostat (PAR Model 362) controlled by a Macintosh II CI computer.

## Results and Discussion

The electrochemical stability range of the PAN-based electrolytes has been determined by running a potential

\* Abstract published in *Advance ACS Abstracts*, March 15, 1994.

(1) Abraham, K. M. In *Applications of Electroactive Polymers*; Scrosati, B., Ed.; Chapman and Hall: London, 1993; p 75.

(2) Croce, F.; Gerace, F.; Dautzenberg, G.; Passerini, S.; Appetecchi, G.; Scrosati, B. *Electrochim. Acta*, submitted.

(3) Croce, F.; Brown, S. D.; Greenbaum, S. G.; Slane, S. C.; Salomon, M. *Chem. Mater.* 1993, 5, 1268.

(4) Tager, A. In *Physical Chemistry of Polymers*; Mir Publishers: 1978.

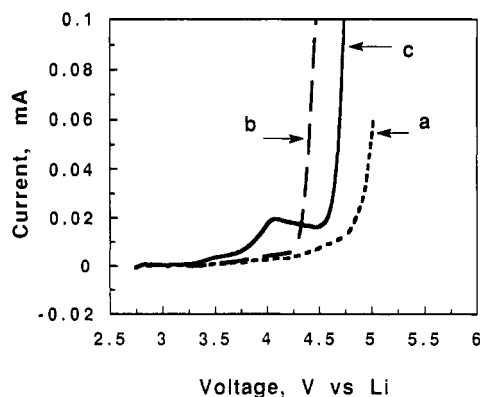


**Figure 1.** Anodic decomposition of the PAN 16/PC 23/EC56.5/LiX 4.5 (sample GE-1) gel electrolytes at room temperature. (a) X = ClO<sub>4</sub><sup>-</sup>; (b) X = AsF<sub>6</sub><sup>-</sup>; (c) X = N(SO<sub>2</sub>CF<sub>3</sub>)<sub>2</sub>. Scan rate: 1 mV s<sup>-1</sup>. Working electrode: SS 304.

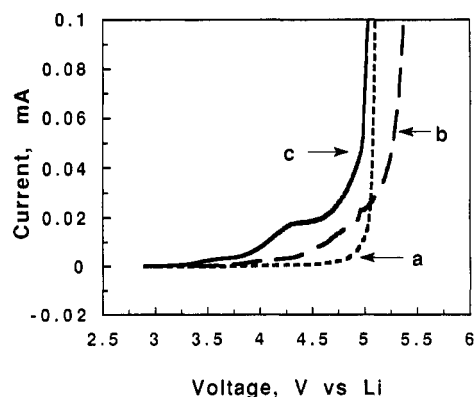


**Figure 2.** Anodic decomposition of the PC 27/EC67.3/LiX 5.3 (sample LE-1) liquid electrolytes at room temperature. (a) X = ClO<sub>4</sub><sup>-</sup>; (b) X = AsF<sub>6</sub><sup>-</sup>; (c) X = N(SO<sub>2</sub>CF<sub>3</sub>)<sub>2</sub>. Scan rate: 1 mV s<sup>-1</sup>. Working electrode: SS 304.

sweep through a three-electrode cell having an "inert" (e.g., stainless steel) working electrode. This technique is routinely used in the electrochemical technology to determine the stability range of a given electrolyte. The anodic and cathodic decomposition limits are in fact determined as the voltages at which current is flowing through the cell.

**Anodic Decomposition.** Figure 1 shows the current-voltage response obtained for cells using GE-1 samples. The trend of these curves suggests that the electrolyte containing LiClO<sub>4</sub> is the most stable since it exhibits a stability up to 4.9 V (curve a). This result is somewhat in contrast with those obtained for the parent liquid electrolytes (Figure 2) where the most stable solution appears to be that based on LiAsF<sub>6</sub>. Indeed, the comparison between the two figures shows that while the anodic stability of LiClO<sub>4</sub> and LiN(SO<sub>2</sub>CF<sub>3</sub>)<sub>2</sub> systems is similar both in PAN gels and in liquid solutions (compare curves a and c), that of LiAsF<sub>6</sub> systems shows dramatic differences, being considerably lower in the gel medium. Probably, this is associable to the decomposition of PAN, as evidenced by a change in coloration acquired during the test. The decomposition of PAN may be catalyzed<sup>5</sup> by the dissociation products of the arsenate anion<sup>6</sup> according to the acid-base equilibrium

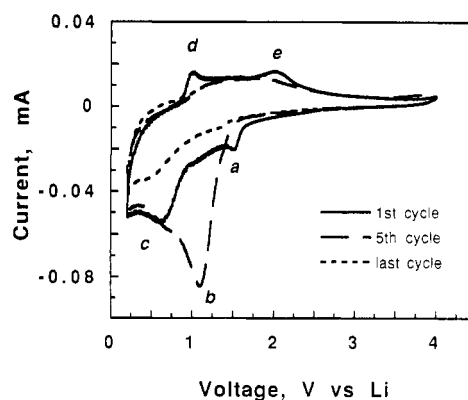


**Figure 3.** Cyclic voltammetry in the voltage range between 0.2 and 4.0 V for the PAN 16/PC 23/EC56.5/LiClO<sub>4</sub> 4.5 (sample GE-1) gel electrolyte at room temperature. Scan rate: 1 mV s<sup>-1</sup>. Working electrode: SS 304.



which is in turn influenced by the chemical environment. In fact, strong polarizing cations like Li<sup>+</sup> shift the equilibrium to the right side.<sup>6</sup> Also the electron-donating ability of the solvent exerts a crucial effect on the degree of dissociation. Indeed, solutions of LiAsF<sub>6</sub> in EC/PC, namely, in strong electron-donating solvents, are very stable, i.e., up to 5.2 V (curve b, Figure 2). In contrast, the addition of PAN, namely, of a poor electron-donating material, should shift the dissociation equilibrium to the right side, this lowering the stability of the gel electrolyte to the observed 4.3 V (curve b, Figure 1).

It is also interesting to note that the anodic curves of LiN(SO<sub>2</sub>CF<sub>3</sub>)<sub>2</sub> systems show, both in liquid and in gel electrolytes, a current peak at 4.1 V (see Figures 1 and 2). The nature of this peak is not yet fully understood. We can only tentatively postulate (also on the basis of further voltammetric analysis not reported here) that it may be due to a partially reversible dissociation of the N(CF<sub>3</sub>SO<sub>2</sub>)<sub>2</sub><sup>-</sup> anion.

The influence on the anodic stability of various parameters, such as salt concentration, PAN concentration and the mixture ratio between EC and PC has been verified and no substantial variation has been found. Only minor differences were observed when changing the content of PAN. In fact, as the molar concentration of PAN increases from 16% to 25%, i.e., passing from samples GE-1 to samples GE-5, the decomposition potential increases only 0.1 V. This minor increment is probably due to a dilution effect of the liquid solvent in the polymer matrix.

**Cathodic Decomposition.** As already discussed, the cathodic decomposition limit can also be determined by cyclic potential sweeps applied to three-electrode cells again using an "inert", stainless steel working electrode.

Figures 3-5 show the current-voltage responses, of lithium perchlorate, arsenate, and imide (samples GE-1) gel electrolytes, respectively, in the first, intermediate, and final steady-state cycles. In all cases three peaks were observed during the first cathodic sweep, namely, at around 1.4 V (a), 1 V (b), and at 0.6 V (c). The second peak is partially masked in the case of the arsenate and perchlorate electrolytes, while it is predominant in the case of the imide electrolyte. In the following anodic scan, two peaks at 1 V (d) and 2 V (e) appear. Peak a is due to the reduction

(5) Pai Verneker, V. R.; Shaha, B. *Macromolecules* 1986, 19, 1851.

(6) Koch, V. R.; Goldman, J. L.; Maurand, J. T. Y.; Mulvaney, M. *Proc. Symp. Lithium Batteries* 1981, 4, 165.

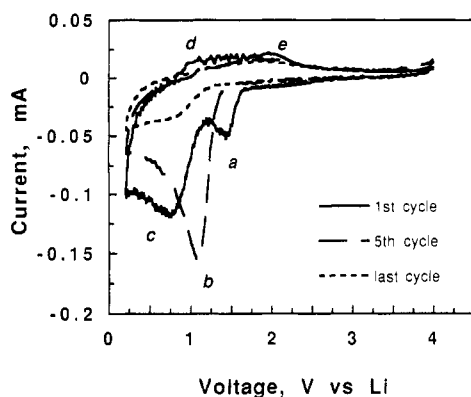


**Figure 4.** Cyclic voltammery in the voltage range between 0.2 and 4.0 V for the PAN 16/PC 23/EC56.5/LiAsF<sub>6</sub> 4.5 (sample GE-1) gel electrolyte at room temperature. Scan rate: 1 mV s<sup>-1</sup>. Working electrode: SS 304.

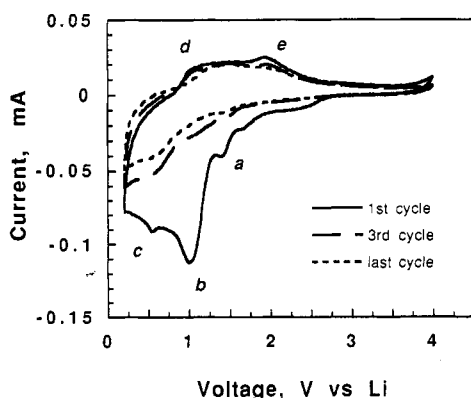


**Figure 5.** Cyclic voltammery in the voltage range between 0.2 and 4.0 V for the PAN 16/PC 23/EC56.5/LiN(SO<sub>2</sub>CF<sub>3</sub>)<sub>2</sub> 4.5 (sample GE-1) gel electrolyte at room temperature. Scan rate: 1 mV s<sup>-1</sup>. Working electrode: SS 304.

of water on stainless steel,<sup>7,8</sup> and, in fact, it disappears on cycling. Furthermore, the intensity of this peak changes for the three salts, depending upon the previous drying process, showing the highest intensity for the lithium arsenate case since this salt was used as received without any further purification (see Experimental Part).

Peak c at lower potential can be assigned to the formation of a lithium-SS alloy.<sup>7,8</sup> Lithium may be stripped from this alloy, as shown by the anodic d peak at 1 V. The correspondence between peaks c and d was further demonstrated by moving the cathodic limit to 0.8 V, so preventing the formation of the alloy: under these conditions the anodic peak d tends to disappear, confirming the assumed correlation between the two peaks.

Peak b for the electrolyte containing imide salt continuously decreases on cycling (see Figure 5), while for perchlorate and arsenate electrolytes the peak reaches its highest intensity at the fifth cycle (see Figures 3 and 4). Koch and co-workers<sup>9</sup> have shown that in arsenate systems a cathodic peak of type b may be assigned to the reduction of the AsF<sub>6</sub><sup>-</sup> anion. The disappearance of this reduction peak after more or less eight cycles (Figure 4) can be explained by SS-electrode passivation. We assume that

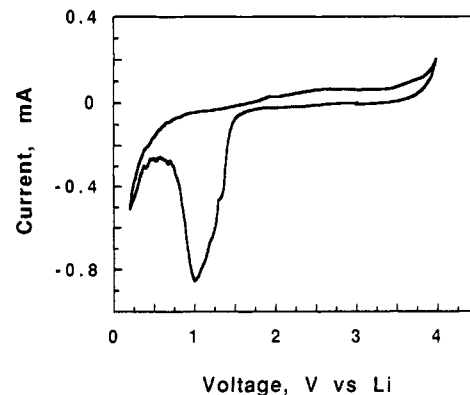


**Figure 6.** Cyclic voltammery in the voltage range between 0.2 and 4.0 V in the first cycle for the PAN 16/PC 23/EC56.5/LiAsF<sub>6</sub> 4.5 (sample GE-1) gel electrolyte at room temperature. Scan rate: 1 mV s<sup>-1</sup>. Working electrode: carbon fiber.

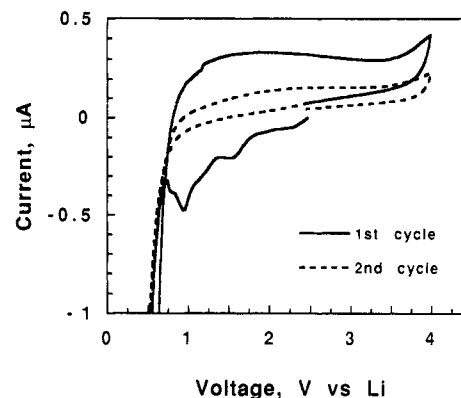


**Figure 7.** Cyclic voltammery in the voltage range between 0.2 and 4.0 V in the first and second cycles for the PAN 16/PC 23/EC56.5/LiAsF<sub>6</sub> 4.5 (sample GE-1) gel electrolyte at room temperature. Scan rate: 1 mV s<sup>-1</sup>. Working electrode: Glassy carbon.

also the peaks around 1 V for the imide and perchlorate electrolytes may be associated to anion reduction.

The above interpretation is supported by results obtained with working electrodes of different nature. In fact, when passing from stainless steel to carbon fibers the current-voltage response presents a broad structure, composed by two peaks centered at 1 V for all the gel samples and the parent liquid electrolytes. Figure 6 shows the response for the electrolyte with lithium hexafluoroarsenate. No peak is obtained at 0.6 V, thus confirming the hypothesis that such a peak may be associated to the formation of a lithium-stainless steel alloy (compare peaks c in Figures 3-5). The broad structure around 1 V is splitted into two well-defined peaks when passing to a glassy carbon working electrode (Figure 7), which disappear completely in the second cycle. The cathodic current flowing at 1.6 V in the first cycle can then be attributed to water reduction,<sup>7,8</sup> while the peak at 1 V should be due to the reduction of the AsF<sub>6</sub><sup>-</sup> anion. The disappearance of the peak in the following cycle is possibly explained as being the result of electrode passivation induced by the reduction products of the arsenate anion.

**Lithium Plating and Stripping Processes.** The characteristics of the lithium plating-stripping process



from PAN-based gel electrolytes has been investigated by cyclic voltammery using a three-electrode cell with a

(7) Jasinski, R. *Adv. Electrochem. Electrochem. Eng.* 1971, 8, 253.

(8) Bohnke, O.; Rousselot, C.; Gillet, P. A.; Truche, C. *J. Electrochem. Soc.* 1992, 139, 1862.

(9) Nanjundiah, C.; Goldman, J. L.; Dominey, L. A.; Koch, V. R. *J. Electrochem. Soc.* 1988, 135, 2914.

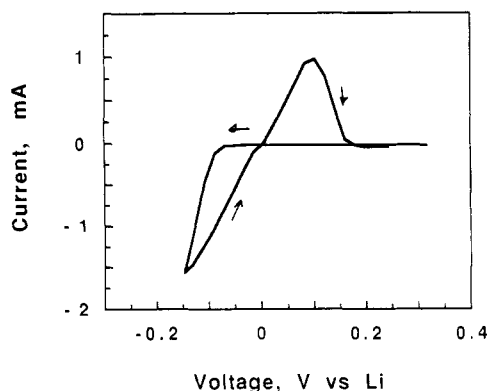


**Figure 8.** Cyclic voltammety for the lithium plating-stripping process in a PAN 21/PC 34.75/EC40/LiClO<sub>4</sub> 4.25 (sample GE-3) gel electrolyte at room temperature. Scan rate: 2 mV s<sup>-1</sup>. Substrate: nickel.

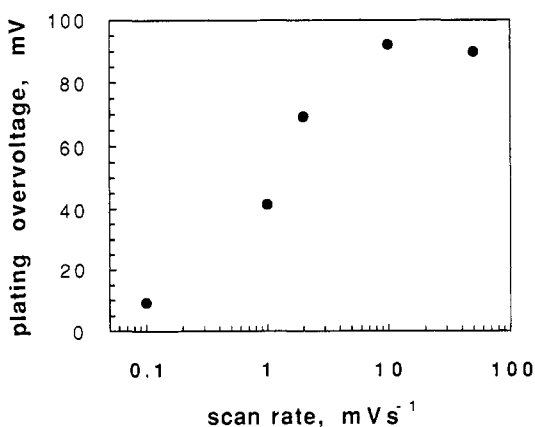


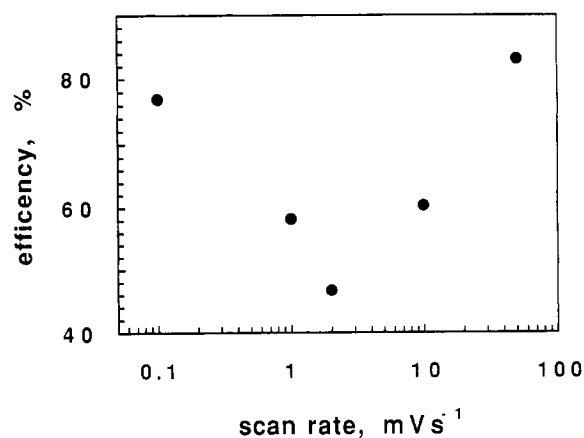
**Figure 9.** Plating overvoltage of the first lithium plating-stripping cycle as a function of the scan rate and at room temperature for a PAN 21/PC 34.75/EC40/LiClO<sub>4</sub> 4.25 (sample GE-3) gel electrolyte cell. Substrate: nickel.

lithium counterelectrode, a lithium reference electrode, and a nickel working substrate. The processes were driven at various scan rates (i.e., at 50, 10, 2, 1, and 0.1 mV s<sup>-1</sup>), and Figure 8 illustrates a typical result obtained at 2 mV s<sup>-1</sup> rate.

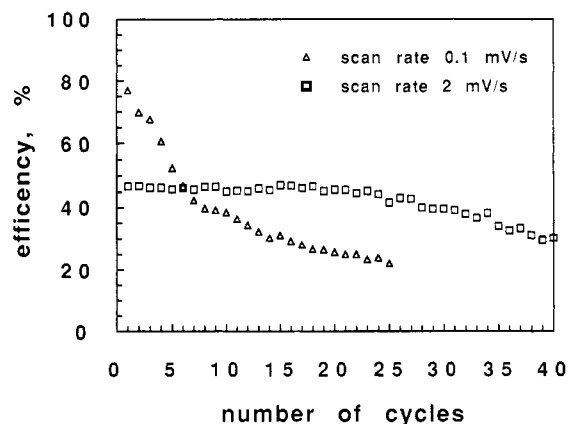
One may clearly note the occurrence of a defined plating overvoltage (70 mV in the case of Figure 8). Figure 9 shows the amount of the observed plating overvoltage as a function of the scan rate for a selected GE-3 electrolyte cell. As expected on kinetic considerations, the lower the scan rate, the lower the overvoltage to be overcome to promote the lithium plating process on the nickel substrate.<sup>10</sup>

Figure 10 reports the efficiency of the process determined at the first plating-stripping cycle. We notice that the efficiency first decreases as the scan rate increases, to reach a minimum at about 2 mV s<sup>-1</sup>, to then increase at higher scan rates.

This particular behavior may be explained only by assuming the occurrence of corrosion phenomena at the lithium interface. Indeed, results obtained in our<sup>2,11</sup> and other laboratories<sup>12</sup> have clearly shown that lithium is attacked and passivated in PAN-based electrolyte cells.



**Figure 10.** Efficiency of the lithium plating-stripping cycles as a function of the scan rates and at room temperature for a PAN 21/PC 34.75/EC40/LiClO<sub>4</sub> 4.25 (sample GE-3) gel electrolyte cell. Substrate: nickel.



**Figure 11.** Efficiency of the lithium plating-stripping cycles at different scan rates and at room temperature for a PAN 21/PC 34.75/EC40/LiClO<sub>4</sub> 4.25 (sample GE-3) gel electrolyte cell. Substrate: nickel.

However, even under these circumstances, the trend of Figure 10 is difficult to explain, since one would have reasonably assumed that if the electrolyte interacts with the freshly deposited lithium generating a passivation layer, the efficiency should accordingly decrease on slowing the scan rate, namely, on increasing the time during which the reaction can occur.

To explain the anomalous behavior of Figure 10, it is necessary to assume that the passivation of the deposited lithium affects only a few electrolyte layers. Under this assumption, the thicker the lithium deposit, the lower the relative percentage of lithium lost, and thus, the higher the efficiency. Accordingly, at very low scan rates, when the amount of plated lithium is high, the efficiency is also high. The efficiency decreases as the rate increases up to a critical value (2 mV s<sup>-1</sup> in the case of Figure 10), namely, when the rate becomes high enough to be competitive with the passivation kinetics. Beyond this value, the time of contact becomes progressively shorter, and thus the efficiency constantly increases, as indeed observed in Figure 10.

This model is confirmed by further experimental results. Figure 11 shows the efficiency measured on progressive lithium-plating cycles run at two scan rates, namely, at 0.1 and 2 mV s<sup>-1</sup>, in a cell using the same electrolyte as in Figure 10. One clearly notices that the efficiency at the low scan rate constantly decreases with cycling (due to a

(10) Bonino, F.; Ottaviani, M.; Scrosati, B. *J. Power Sources* 1987, 20, 333.

(11) Croce, F.; Scrosati, B. *J. Power Sources* 1993, 44, 9.

(12) Abraham, K. M.; Alamgir, M. *J. Power Sources* 1993, 44, 195.

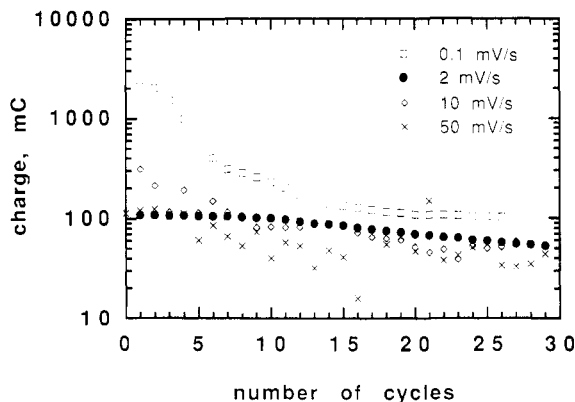


**Figure 12.** Charge of lithium plated during plating-stripping tests run at various scan rates and at room temperature for a PAN21/PC 34.75/EC40/LiClO<sub>4</sub> 4.25 (sample GE-3) gel electrolyte cell. Substrate: nickel.

progressive increase of contact time) while that at scan rate which critically competes with the passivation kinetics (i.e., 2 mV s<sup>-1</sup>) the efficiency remains practically constant. Figure 12 shows the charge involved in the plating lithium process as the function of the number of cycles and of the value of the scan rate. Again, almost no variations are observed for cycles run at the critical scan rate (2 mV s<sup>-1</sup>)

while progressive decays are observed both at lower and at higher scan rates.

### Conclusions

The dimensional stability (plasticlike consistence up to 75 °C) together with the high conductivity at ambient and subambient temperature makes the family of PAN-based gel electrolytes suitable for use in room-temperature electrochemical devices. However, the low cathodic stability and the poor plating-stripping efficiency may affect applicability for batteries using a lithium metal anode. On the other hand, the high anodic stability shown by the samples using LiClO<sub>4</sub> and LiN(SO<sub>2</sub>CF<sub>3</sub>)<sub>2</sub> lithium salts makes these gel electrolytes quite suitable for the alternative lithium-metal-free "rocking chair" systems.

**Acknowledgment.** G.D. and S.P. wish to thank Arcotronics Italia and Società Industriale Accumulatori Srl for Research Fellowships. We wish to thank also Prof. M. Duclot for kindly providing the carbon fiber electrodes and the European Office of Aerospace Research and Development of the U.S. Force, Contract No. SPC-93-4033 for financial support.